Seismic Discrimination of Nuclear Explosions at the Lobnor Test Site

Yu. F. Kopnichev, O. M. Shepelev, and I. N. Sokolova

Schmidt United Institute of Physics of the Earth, Russian Academy of Sciences,
Bol'shaya Gruzinskaya ul. 10, Moscow, 123810 Russia

Received April 6, 2000

Abstract—The structure of short-period seismic fields was studied from data on underground nuclear explosions at the Lobnor test site and earthquakes in western China recorded by four seismic stations in Kazakhstan. As many as 78 records of events with magnitudes m_b = 3.4–6.5 obtained between 1969 and 1999 at epicentral distances of 540–2300 km were considered. Amplitude ratios of various phases of P and S waves processed by four narrow-band filters within a frequency range of 0.5–6.0 Hz were analyzed. Optimal parameters and frequency bands providing the most efficient discrimination between explosions and earthquakes are determined for each station.

INTRODUCTION

The problem of seismic discrimination between underground nuclear explosions (UNEs) and earthquakes has become even more important after the nuclear tests carried out by India and Pakistan in 1998. This problem is most complicated for comparatively weak events ($m_b < 4.5$) and at regional distances (from a few hundreds up to $2–2.5 \times 10^3$ kilometers). At such distances, regular seismic waves propagate in the Earth's crust and upper mantle, and the inhomogeneity of the velocity and attenuation fields in the lithosphere and asthenosphere have a strong effect on their amplitude characteristics [Antonova *et al.*, 1978; Kopnichev, 1985; Kopnichev and Arakelyan, 1988; Kim *et al.*, 1993]. Considerable variations in short-period wave field characteristics due to the heterogeneity of the medium require that records of explosions and earthquakes from relatively small areas be compared. In this case, in order to obtain a more or less representative dataset, it is necessary to use records accumulated during a relatively long period of observations. Variations in the characteristics of instruments used in different time periods can further complicate the analysis of such data. In this work, we made an attempt to remove this difficulty by unification of diverse seismic data.

Below, we describe the results of studies on the discrimination between nuclear explosions at the Lobnor test site (LTS) in northwestern China and near earthquakes. The main goal of the work is a detailed analysis of the structure of short-period seismic wave fields from the events in this area and its application to the determination of parameters and frequency ranges that are most advantageous to the discrimination between nuclear explosions and earthquakes from records of different seismic stations.

The distinctions of our work from recent foreign publications [Hartse *et al.*, 1997; Fan and Lay, 1998a, 1998b, 1998c; Phillips *et al.*, 1999; Taylor *et al.*, 1999] are as follows. First, data on explosions and earthquakes covering a considerably longer time period (1969–1999) were used. Second, records of seismic events obtained at stations that previously had not been used for discrimination (PDG) were processed. Third, we carried out a more detailed analysis of time–frequency fields in order to reveal the most efficient discriminants.

In contrast to the work by Kedrov and Lyuke [1999], we mainly used records obtained at stations located closer to the LTS and events from a relatively small area of western China where the test site is located (Fig. 1). In addition, records obtained with diverse recording instruments were processed with the help of narrow-band frequency filters, thereby eliminating the effects caused by differences between instrumental frequency characteristics. All these factors substantially reduced the scatter in data.

OBSERVATION SYSTEM AND DATA USED

We analyzed the records obtained at stations of the Joint seismological expedition of the Schmidt United Institute of Physics of the Earth, Russian Academy of Sciences (TLG, PDG); the Institute of Geophysical Research, National Nuclear Center of Kazakhstan (MAK, ZRN); and the Institute of Seismology, National Academy of Sciences of Kazakhstan (PDG). A map showing the position of the seismic stations and epicenters of the events studied is presented in Fig. 1.

We processed 78 records of 47 events (29 earthquakes and 18 UNEs) from the (39°–43° N, 86°–92° E) area. The parameters of the events are presented in Table 1. The events ranged in magnitude m_b from 3.4 to 6.5 and in epicentral distance from 540 to 2300 km.
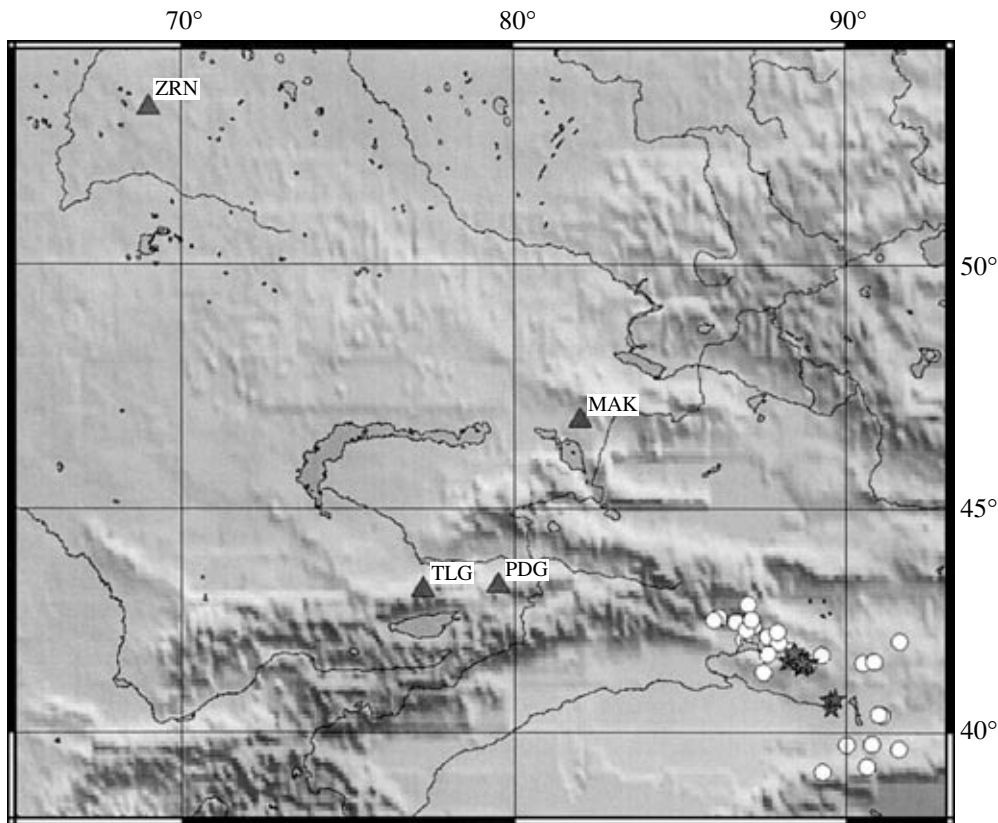
Fig. 1. Map of the study area. Triangles are seismic stations; circles and stars are the epicenters of earthquakes and explosions.

INSTRUMENTATION

We used data obtained with the help of various types of instrumentation, which made it possible to cover a relatively long time interval (1969–1999). The characteristics of the seismic stations are presented in Table 2.

The ASS-6/12 magnetic recording complex [Brulev *et al.*, 1980]. Each station of magnetic recording is equipped with three SM-3 (three-component) seismometers with a natural period of 1.5 s. The –3-dB frequency range is 0.5–16 Hz with a recording speed of 0.5 mm per second. In order to convert the information recorded on a magnetic tape at the ASS-6/12 recording stations into graphic form on photographic paper or into a digital format, the VSS-3/6 reproduction station was used. The records used in this work were digitized at frequencies of 20 and 25 Hz.

SKM-3 seismometers. A set of seismometers is used, which consists of two horizontal and one vertical seismometers with a natural period of 1.6 s are used for three-component recording [Aranovich *et al.*, 1974]. The –3-dB working frequency range of the instrumentation is 0.5–9.0 Hz. We used seismograms recorded on photographic paper with a time base of 120 mm/min. The seismograms were scanned and digitized with the help of special software with a frequency of 40 Hz.

Frequency-selective seismic (FSS) stations. We used data obtained on FSSS analogue short-period

instrumentation [Zapol'skii, 1971]. An FSS station performs the continuous time-spectral analysis of the ground motion velocity in the recording process with a time base of 60 mm/min.

Digital stations. We also used data obtained with the help of the three-component digital stations REFTEK and GSN, installed in Kazakhstan (KAZNET) [Belyashova and Malakhova, 2000]. The stations are equipped with the STS-2, CMG-3, and CMG-40T seismometers with bandpasses of 0.008–45 Hz (STS-2) and 0.03–80 Hz (CMG-3 and CMG-40T). The data were digitization at frequencies of 20 and 40 Hz.

The TLG-station records were obtained by the analog SKM-3, FSS and ASS-6/12 stations and on the digital REFTEK station. The records of the ZRN and MAK stations were obtained with the REFTEK and GSN (MAK) instruments, and the records of the PDG station, with the SKM-3 and REFTEK instruments.

DATA PROCESSING METHOD

All seismic data, except the data obtained with the FSS stations, were digitized. In order to exclude the effects related to differences between the spectral characteristics of the records, which can be caused by various factors (variations in source radiation spectra, inho-

Table 1. Parameters of earthquake and explosion in the LTS area

Date	Time	φ°, N	λ°, E	Depth, km	Type	m_b	M_S	M_L	Stations
September 29, 1969	8:40:12.4	40.722	89.515	0	UNE	4.3			TLG
January 15, 1973	14:42:07.8	40.387	91.055	13	EQ	4.7			TLG
January 23, 1973	11:31:48.3	40.409	90.96	33	EQ	4.9			TLG
June 27, 1973	3:59:51.0	40.559	89.532	33	UNE	4.8			TLG
October 17, 1976	5:00:03.8	41.64	88.21	33	UNE	4.90			TLG
November 17, 1976	6:00:17.600	40.76	89.66	33	UNE	4.60			TLG
October 14, 1978	1:00:02.7	41.488	88.637	33	UNE	4.9			TLG
February 2, 1979	1:08:41.0	39.719	90.754	33	EQ	5.0			TLG
May, 4, 1983	5:00:02.0	41.63	88.31	0	UNE	5.0			TLG
June 9, 1983	6:25:16.000	39.7	90	33	EQ	4.40			TLG
October 3, 1984	5:59:57.900	41.54	88.67	0	UNE	5.40			TLG
June 5, 1987	4:59:58.300	41.584	88.737	0	UNE	6.2	4.4		TLG
September 29, 1988	7:00:03.1	41.75	88.474	33	UNE	4.7			TLG
May 26, 1990	7:59:57.800	41.566	88.688	0	UNE	5.40			TLG, PDG
December 18, 1991	13:44:03.900	41.37	87.5	33	EQ	4.50			TLG
May 21, 1992	4:59:57.500	41.604	88.81	0	UNE	6.5	5.0		PDG
September 25, 1992	7:59:59.9	41.763	88.387	10	UNE	5.0			TLG
April 14, 1993	8:31:09.700	42.904	87.045	33	EQ	4.40		4.80	ZRN
June 10, 1994	6:25:58.000	41.54	88.74	0	UNE	5.8	4.1		PDG
October 7, 1994	3:25:57.900	41.58	88.77	0	UNE	5.9	4.5		MAK
December 26, 1994	16:58:46.1	41.594	88.833	10	EQ	4.6			TLG, ZRN
March 18, 1995	18:02:36.600	42.422	87.199	22	EQ	5.20		5.40	ZRN
May 15, 1995	4:05:57.900	41.59	88.82	0	UNE	6.0	5.00		ZRN
July 5, 1995	23:38:48.900	42.513	86.678	33	EQ	4.50			MAK, TLG
August 2, 1995	11:59:43.900	41.631	88.447	10	EQ	4.10			MAK, ZRN
August 17, 1995	0:59:57.900	41.56	88.79	0	UNE	5.9	5.7		ZRN, PDG
December 12, 1995	17:31:16.800	42.117	86.911	33	EQ	4.30			TLG, ZRN
February 20, 1996	8:05:07.1	41.59	90.49	14	EQ	3.9			MAK
March 20, 1996	2:11:21.900	42.182	87.627	24	EQ	4.80			MAK, ZRN
May 10, 1996	11:26:04.000	41.868	88.234	22	EQ	3.80			MAK
June 8, 1996	2:55:58.00	41.60	88.66	0	UNE	5.7	4.4		MAK, ZRN, TLG
July 29, 1996	1:48:57.800	41.824	88.42	0	UNE	4.90			MAK, TLG
August 24, 1996	12:15:26.200	39.606	91.569	33	EQ				TLG, ZRN, MAK
February 8, 1997	17:12:09.100	42.34	86.99	10	EQ	4.60			TLG
May 13, 1997	21:13:00.300	39.197	90.598	33	EQ	3.40			TLG
May 27, 1997	1:56:24.800	42.618	86.158	22	EQ	4.90			TLG, ZRN
June 8, 1997	20:25:53.600	39.061	89.276	33	EQ	4.70			MAK, TLG, ZRN
February 7, 1998	22:42:44.000	42.554	86.008	33	EQ	4.1			MAK, TLG, ZRN, PDG
October 20, 1998	18:39:23.2	42.561	87.148	33	EQ	4.7			TLG, ZRN, PDG
January 25, 1999	19:50:05.000	42.076	91.587	33	EQ	4.80			TLG, MAK, ZRN, PDG
January 27, 1999	6:25:01.800	41.624	88.36	33	EQ	4.50			TLG, ZRN, PDG
January 30, 1999	3:51:05.400	41.674	88.463	23	EQ	5.90	5.30	5.50	TLG, ZRN, PDG
April 29, 1999	5:27:55.2	41.624	90.823	33	EQ	4.3			PDG
May 1, 1999	13:48:52.00	42.037	87.959	21	EQ	4.20			TLG, PDG
May 17, 1999	4:52:34.0	42.284	87.917	33	EQ	4.2			MAK
July 22, 1999	21:01:26.0	41.786	87.638	10	EQ				ZRN, PDG
October 18, 1999	2:42:20.3	41.766	89.248	33	EQ	4.7	5.0		TLG, MAK, PDG

Note: EQ stands for earthquake.
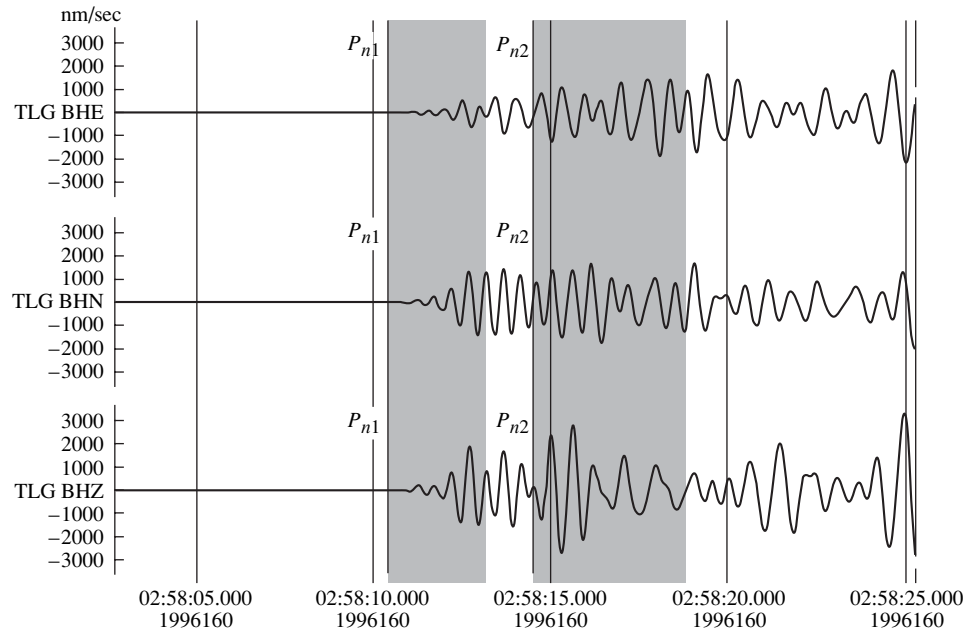
Fig. 2. Identification example of the P_{n1} and P_{n2} wave phases. The June 8, 1996 UNE TLG record (Δ = 955 km; channel centered at 1.25 Hz).

mogeneity of the seismic wave attenuation field in the lithosphere and asthenosphere, and different frequency responses of instruments), all measurements were carried out only after the records had been processed with the help of narrow-band filters. The general frequency range was determined by instrumental characteristics, magnitudes, and epicentral distances for most of the events selected. Measurements could not be made beyond this range because of low signal/noise ratios. Filters with center frequencies of 0.6, 1.25, 2.5 and 5 Hz and with a bandpass of 2/3 of an octave at a level of –3 dB from the maximum were used. The filter characteristics were chosen in such a way as to ensure comparison with analog data from the FSS stations. Recorded displacements (SKM) were not converted into velocities (FSS, ASS-6/12, CMG-3, CMG-40T,

and STS-2) or vice versa, because this difference between the data is inessential for the amplitude ratios if narrow-band frequency filters are used [Rogers *et al.*, 1997].

The maximum amplitudes of the P_{n1}, P_{n2}, S, S_n, S_m, and Lg waves and Lg coda were measured. The P_{n1} phase was identified as a first visible arrival. The P_{n1} amplitude maximum was measured within the first two-thirds of the time interval preceding the P_{n2} phase (Fig. 2). The traveltime curve of the P_{n2} phase was constructed relative to the P_{n1} phase (Fig. 3). As a rule, the P_{n2} phase are reliably recognized in frequency ranges centered at 1.25 and 2.5 Hz, and more rarely, in other frequency ranges (depending on the epicentral distance). The identification of this phase is unreliable

Table 2. Parameters of seismic stations

Station		Coordinates		Elevation, m	Geological setting	Instrumentation	
name	code	$\varphi°$, N	$\lambda°$, E			type	bandpass, Hz
Makanchi	MAK	46.808	81.977	600	Andesite	STS-2	0.008–45
Podgornoe	PDG	43.327	79.485	1300	Granite	SKM-3	0.5–9
						CMG-40T	0.03–80
						CMG-3	0.03–80
Talgar	TLG	43.249	77.223	1120	Granite	FSS	0.022–45
						ASS-6/12	0.5–16
						CMG-3	0.03–80
Zerenda	ZRN	52.951	69.004	420	Granite	STS-2	0.008–45

$t - t(P_{n1})$, s
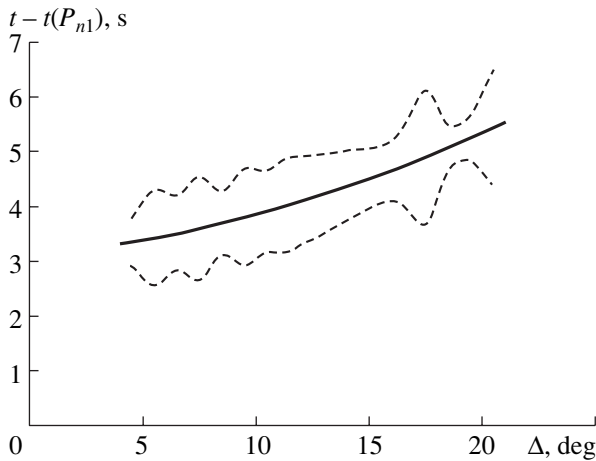
Fig. 3. The P_{n2} traveltime curve (solid line) and rms deviations averaged over 1-degree intervals (dotted lines).

without application of frequency filters. At the epicentral distances considered, the P_{n2} arrival onset varies from 2 to 7 s after the first arrival time. The P_{n2} amplitude was measured in a 5-s time interval beginning from its arrival in the traveltime curve.

Maximal amplitudes were also measured in a group denoted here as S_m (this group is recorded in the time interval between the S_n and Lg arrivals). The characteristic feature of this group is that its level relative to the P_n wave, other factors being the same, characterizes the integral attenuation of S waves in the lithosphere and asthenosphere in the epicentral area of the event considered [Kopnichev and Arakelyan, 1988]. If the amplitude in the S_n group was highest in the time interval considered, S_m was considered to coincide with S_n. The S_m arrival time was determined independently for different components, i.e., different components actually yielded evidence of different waves, formally denoted as S_m.

The Lg coda was measured in time intervals $t_i \pm \Delta t$, where t_i takes the values 300, 450, and 600 s, and the Δt values were equal to 10 s for frequencies of 0.6 and 1.25 Hz and 5 s for 2.5 and 5 Hz (the time t is measured from the radiation onset time in the source). These phases were denoted as s300, s450, and s600, respectively.

In those cases, when wave phases could not be identified or when the identified phases were very weak, the amplitudes of the related waves were not determined. Also, coda amplitudes were not measured if the oscillations did not attenuate or reached in amplitude the background level throughout the pertinent time interval.

In this work, we did not use the amplitude characteristics of the Pg group because it could be identified at all stations within the frequency range considered.

Surface wave amplitudes also were not measured because they are unrecognizable from the records of

high-frequency FSS channels at the distances considered.

Decimal logarithms of the amplitude ratios of the study wave groups to the P_{n1} and P_{n2} waves measured from the same (vertical or horizontal) component were analyzed. For the sake of simplicity, we omit the repeating symbols: for example, the $\log(A_{Lg}/AP_{n2})$ value will be denoted as Lg/P_{n2}, and so on. The azimuthal transformation of the horizontal coordinate axes was not carried out, because some data, particularly older records, do not allow such a transformation to be correctly carried out.

The following characteristics of the logarithmic amplitude ratios were analyzed for discrimination purposes: (1) sampled averages from explosions and earthquakes; (2) sample dispersions; and (3) the discrimination quality coefficient (DQC)

$$K_{qd} = \frac{\overline{X}_{eq} - \overline{X}_{ex}}{\sqrt{S_{eq}} + \sqrt{S_{ex}}},$$

where $\overline{X}_{eq}$ and $\overline{X}_{ex}$ are sampled averages, and S_{eq} and S_{ex} are dispersions for earthquakes and explosions, respectively (obviously, the larger the its absolute value, the lower the probability of error); (4) the threshold value allowing the discrimination between explosions and earthquakes occurs; and (5) the percentage of errors of the "false alarm" or "target missing" type. Here, the "false alarm" is the number of misidentified explosions (i.e., earthquakes) relative to the total number of events identified as explosions, and the "target missing" is the number of explosions recognized as earthquakes relative to the total number of explosions for which the pertinent parameters were measured.

ANALYSIS OF THE EXPERIMENTAL DATA

TLG station. We processed TLG records of 33 events at epicentral distances ranging from 720 to 1250 km (20 earthquakes and 13 UNEs). All of the aforementioned phases (P_{n1}, P_{n2}, S_n, S_m, Lg, s300, s450, and s600) were measured in accordance with the technique described above. The s300 phase was excluded from further analysis because it could not be identified from most records.

The signal/noise ratio within the frequency ranges considered had a significant effect on the number of measurements. Moreover, the digitized SKM seismograms were not used for measurements within a frequency range around 5 Hz, because the digitization errors dramatically increased at filter frequencies higher than 3 Hz. Overall, 21, 31, 30, and 13 records were processed in the respective frequency ranges centered at 0.6, 1.25, 2.5, and 5 Hz.

All statistical calculations used samples, without approximating the distribution curves. As seen from Tables 3.1 and 3.2 and from Fig. 4, the highest DQC

values and virtually complete absence of errors are characteristic of the S_n/P_{n2}, S_m/P_{n2}, and Lg/P_{n2} ratios for all components in a channel centered at 5 Hz. However, as is evident from the number of the events processed, approximately 60% of records were rejected from the analysis for the reasons mentioned above.

The N–S s600/P_{n2} ratio was found to be a more reliable parameter in a 1.25-Hz central frequency range. The pertinent N–S component is close to the tangential direction because the azimuths of the records considered varied within a range of 92°–110°. The DQC for this ratio is 1.68. Averages for explosions and earthquakes are, respectively, –0.789 and –0.325, and the corresponding variances are 0.0087 and 0.033.

MAK station. The MAK records of 14 events at epicentral distances of 570 to 1100 km were processed (11 earthquakes and 3 UNEs).

The signal/noise ratio at this station is significantly higher than at the TLG station. For this reason, records of nearly all study events were processed in all frequency ranges considered. The discrimination is best for the 2.5-Hz central frequency filtering (Fig. 5) and is somewhat less effective in the case of the channel centered at 5 Hz. On the whole, the discrimination potential of the MAK records is higher compared to the TLG station, because a higher signal/noise ratio at frequencies most favorable for the discrimination makes it possible to process a larger number of events.

Data on the efficiency of the discrimination are presented in Table 4 and Fig. 6. The azimuths of the study events ranging from 121° to 144°, the processing results from horizontal components are auxiliary. The vertical component provides the best quality of discrimination by the s450/P_{n2} and s300/P_{n2} parameters in the ranges centered at 2.5 and 5 Hz, respectively. The respective QDC values are 4.68 and 3.22. The averages

Table 3.1. Discrimination errors: TLG station, Z channel

Filter, Hz	Parameter	S_n/P_{n1}	S_m/P_{n1}	Lg/P_{n1}	c450/P_{n1}	c600/P_{n1}	S_n/P_{n2}	S_m/P_{n2}	Lg/P_{n2}	c450/P_{n2}	c600/P_{n2}
0.6	Threshold value	0.664	1.038	1.341	0.631	0.050	0.181	0.515	0.738	0.112	–0.372
	Target missing	0.556	0.222	0.222	0.286	0.333	0.600	0.455	0.455	0.222	0.833
	False alarm	0.333	0.417	0.364	0.375	0.333	0.333	0.400	0.250	0.300	0.667
1.25	Threshold value	0.104	0.491	0.555	–0.254	–0.771	0.067	0.151	0.190	–0.355	–1.034
	Target missing	0.875	0.692	0.692	0.727	0.400	0.625	0.750	0.833	0.200	0.000
	False alarm	0.667	0.556	0.556	0.400	0.400	0.571	0.500	0.600	0.429	0.000
2.5	Threshold value	0.030	0.256	0.370	–0.484	–0.692	–0.382	–0.041	0.040	–0.558	–1.024
	Target missing	0.375	0.300	0.444	0.375	0.250	0.375	0.200	0.333	0.125	0.250
	False alarm	0.615	0.588	0.643	0.583	0.667	0.167	0.273	0.571	0.563	0.500
5	Threshold value	–0.454	–0.308	–0.387	–0.926	–1.260	–0.666	–0.465	–0.610	–1.078	–1.220
	Target missing	0.500	0.333	0.500	0.500	1.000	0.000	0.000	0.000	0.000	1.000
	False alarm	0.500	0.333	0.500	0.500	1.000	0.000	0.000	0.000	0.000	1.000

Table 3.2. Discrimination errors: TLG station, N–S channel

Filter, Hz	Parameter	S_n/P_{n1}	S_m/P_{n1}	Lg/P_{n1}	c450/P_{n1}	c600/P_{n1}	S_n/P_{n2}	S_m/P_{n2}	Lg/P_{n2}	c450/P_{n2}	c600/P_{n2}
0.6	Threshold value	0.937	1.171	1.431	1.076	0.242	0.805	0.915	1.259	0.625	0.026
	Target missing	0.500	0.500	0.250	0.333	0.333	0.143	0.429	0.571	0.167	0.000
	False alarm	0.333	0.333	0.400	0.333	0.333	0.333	0.200	0.400	0.167	0.000
1.25	Threshold value	0.669	0.714	0.839	0.147	–0.517	0.478	0.713	0.806	0.075	–0.645
	Target missing	0.667	0.857	0.857	0.667	0.250	0.714	0.125	0.250	0.286	0.000
	False alarm	0.667	0.750	0.750	0.667	0.400	0.714	0.364	0.500	0.545	0.000
2.5	Threshold value	–0.093	0.242	0.280	–0.592	–1.280	–0.027	0.232	0.304	–0.496	–1.395
	Target missing	0.625	0.625	0.857	0.286	0.000	0.250	0.250	0.429	0.143	0.333
	False alarm	0.250	0.500	0.800	0.444	0.000	0.400	0.538	0.556	0.600	0.333
5	Threshold value	–0.492	–0.253	–0.298	–0.575	–0.548	–0.550	–0.423	–0.386	–1.019	–0.991
	Target missing	0.500	0.000	0.000	0.000	0.000	0.000	0.000	0.000	0.500	1.000
	False alarm	0.500	0.000	0.000	0.000	0.000	0.000	0.000	0.000	0.500	1.000
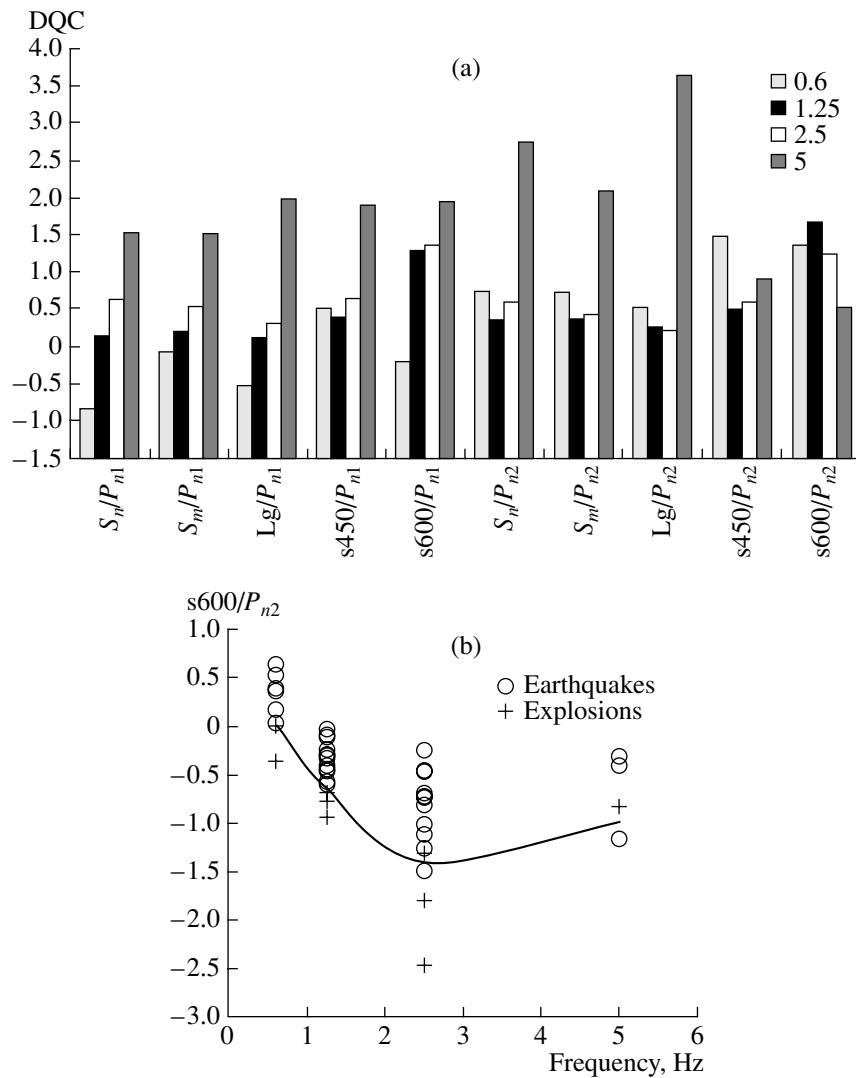
Fig. 4. (a) DQC values for various types of the *Z*-channel amplitude ratios (the numbers under this and similar figures denote central frequencies). (b) Distribution of the s600/P_{n2} ratio for explosions and earthquakes. TLG station, N–S channel.

of the first parameter are –2.62 for explosions and –1.24 for earthquakes; the respective variances are 0.084 and 0.264. The second parameter has respective averages of –1.78 and –0.704 and respective variances of 0.025 and 0.03. However, as can be seen from Table 4, other parameters of the X/P_{n2} type are also effective in the same frequency ranges.

ZRN station. The ZRN records of 18 events were processed (15 earthquakes and 3 UNEs). Their epicentral distances ranged from 1700 to 2300 km. The s300 and s450 phases were not analyzed because they could not be identified by the technique chosen. The ZRN records yield no attenuation in the time windows of these phases, which is related to larger epicentral distances as compared with the other stations.

Overall, 13, 18, 16, and 7 records were processed in the respective frequency ranges centered at 0.6, 1.25, 2.5, and 5 Hz. The records of $m_b < 4.8$ events in the

range centered at 5 Hz were unprocessed. Due to the insufficient amount of data, results of measurements in this frequency range were rejected from the further analysis.

The data on the efficiency of the discrimination are presented in Table 5 and Fig. 7. The records of the channel centered at 2.5 Hz provided the best discrimination. As seen from Table 5, the recognition of explosions was errorless at this frequency.

The results of data processing for the horizontal components were considered auxiliary (the azimuths ranged from 117° to 127°). The S_m/P_{n2} ratio in the range centered at 2.5 Hz is the best discriminant for the vertical component. Its DQC is 2.33, its averages are –1.21 for explosions and –0.57 for earthquakes, and the respective variances are 0.0047 and 0.042. The S/P_{n2} DQC in the range centered at 1.25 Hz is 3.33, but the *S* phase is sometimes unreliably identified in this range.
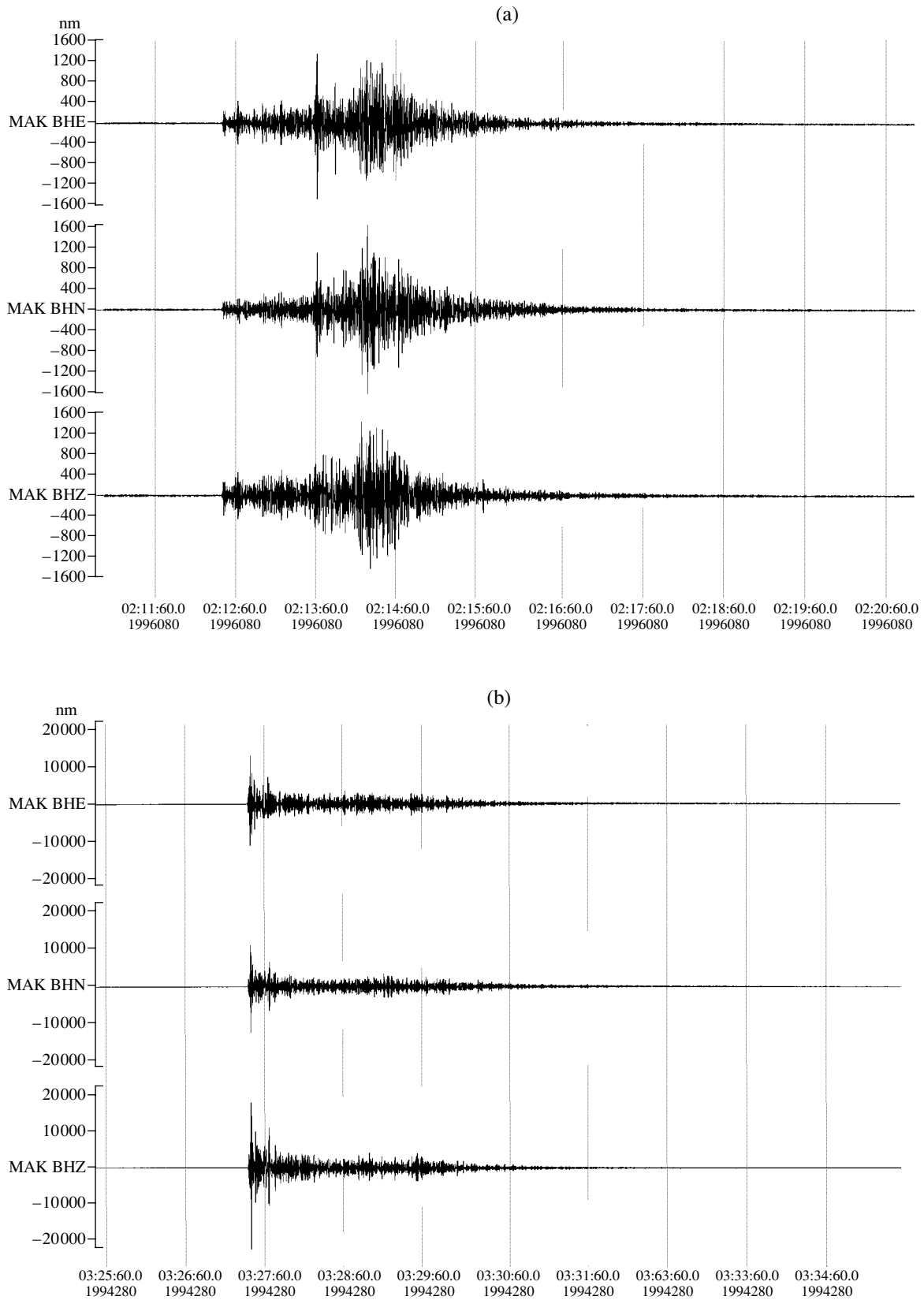
Fig. 5. Seismograms of (a) the March 20, 1996 earthquake, Δ = 677 km, and (b) the October 7, 1994 UNE, Δ = 785 km (MAK station, channel centered at 2.5 Hz). The vertical lines mark 1-min intervals.

Table 4. Discrimination errors: MAK station, *Z* channel

Filter, Hz	Parameter	S_n/P_{n1}	S_m/P_{n1}	Lg/P_{n1}	c450/P_{n1}	S_n/P_{n2}	S_m/P_{n2}	Lg/P_{n2}	c300/P_{n2}	c450/P_{n2}	c600/P_{n2}
0.6	Threshold value	0.679	0.926	1.147	0.289	0.172	0.246	0.772	0.142	−0.405	−0.698
	Target missing	1.000	1.000	1.000	1.000	0.000	0.667	0.333	1.000	1.000	0.667
	False alarm	1.000	1.000	1.000	1.000	0.000	0.500	0.333	1.000	1.000	0.667
1.25	Threshold value	0.304	0.356	0.676	−0.690	−0.295	−0.243	0.048	−0.411	−1.118	−1.315
	Target missing	0.333	0.333	0.333	0.667	0.333	0.333	0.333	0.333	0.000	0.000
	False alarm	0.600	0.500	0.333	0.500	0.333	0.333	0.333	0.333	0.000	0.000
2.5	Threshold value	0.016	0.003	0.047	−1.204	−0.788	−0.722	−0.658	−1.058	−1.781	−2.130
	Target missing	0.333	0.333	0.333	0.000	0.333	0.000	0.000	0.000	0.000	0.000
	False alarm	0.333	0.333	0.333	0.000	0.333	0.000	0.000	0.000	0.000	0.000
5	Threshold value	−0.179	−0.061	−0.123	−1.562	−0.838	−0.673	−0.752	−1.300	−2.155	−2.138
	Target missing	0.333	0.000	0.000	0.333	0.000	0.000	0.000	0.000	0.000	0.000
	False alarm	0.333	0.000	0.000	0.333	0.000	0.000	0.000	0.000	0.000	0.000

Table 5. Discrimination errors: ZRN station, *Z* channel

Filter, Hz	Parameter	S/P_{n1}	S_n/P_{n1}	S_m/P_{n1}	Lg/P_{n1}	c600/P_{n1}	S/P_{n2}	S_n/P_{n2}	S_m/P_{n2}	Lg/P_{n2}	c600/P_{n2}
0.6	Threshold value	−0.442	−0.619	−0.373	−0.054	–	−0.303	−0.129	0.008	0.176	–
	Target missing	1.000	1.000	1.000	0.000	–	0.333	1.000	0.333	0.333	–
	False alarm	1.000	1.000	1.000	0.000	–	0.500	1.000	0.667	0.714	–
1.25	Threshold value	−0.564	−0.697	−0.564	−0.476	−0.599	−0.553	−0.825	−0.556	−0.450	−0.608
	Target missing	0.333	0.000	0.333	0.667	1.000	0.000	1.000	0.333	0.333	1.000
	False alarm	0.333	0.000	0.500	0.500	1.000	0.000	1.000	0.333	0.333	1.000
2.5	Threshold value	–	−0.778	−0.695	–	−1.067	–	−1.082	−1.004	–	−1.411
	Target missing	–	0.000	0.000	–	0.000	–	0.000	0.000	–	0.000
	False alarm	–	0.000	0.000	–	0.000	–	0.000	0.000	–	0.000
5	Threshold value	–	–	−0.772	–	−1.275	–	–	−1.006	–	−1.456
	Target missing	–	–	0.000	–	0.000	–	–	0.000	–	0.000
	False alarm	–	–	0.000	–	0.000	–	–	0.000	–	0.000

Table 6. Discrimination errors: PDG station, *Z* channel

Filter, Hz	Parameter	S_n/P_{n1}	S_m/P_{n1}	Lg/P_{n1}	c300/P_{n1}	c450/P_{n1}	S_n/P_{n2}	S_m/P_{n2}	Lg/P_{n2}	c300/P_{n2}	c450/P_{n2}
0.6	Threshold value	−0.056	−0.056	0.486	−0.199	−0.770	0.661	0.346	0.833	0.299	−0.241
	Target missing	1.000	1.000	0.000	1.000	0.000	1.000	0.500	0.000	1.000	0.000
	False alarm	1.000	1.000	0.000	1.000	0.000	1.000	0.500	0.000	1.000	0.000
1.25	Threshold value	0.186	0.104	0.350	−0.404	−1.158	0.032	0.052	0.549	0.016	−0.934
	Target missing	0.500	0.500	0.500	1.000	0.000	0.500	0.500	0.500	0.500	0.000
	False alarm	0.667	0.500	0.500	1.000	0.000	0.500	0.667	0.667	0.667	0.000
2.5	Threshold value	−0.043	0.086	0.150	−0.615	−1.683	−0.255	−0.114	0.129	−0.659	−1.618
	Target missing	0.500	0.500	0.500	0.500	0.500	0.000	0.000	0.500	1.000	0.500
	False alarm	0.667	0.667	0.800	0.667	0.500	0.000	0.000	0.500	1.000	0.500
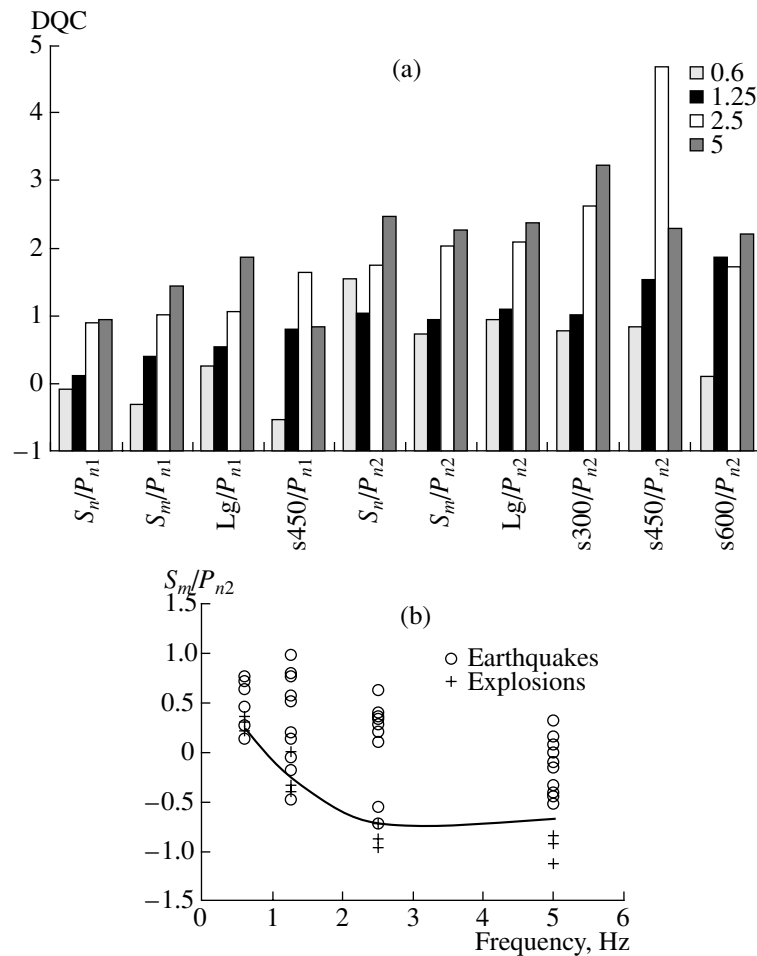
Fig. 6. (a) DQC values for various types of amplitude ratios. (b) Distribution of the S_m/P_{n2} ratio for explosions and earthquakes. MAK station, Z channel.

PDG station. We processed 13 PDG records (9 earthquakes and 4 UNEs). The epicentral distances ranged from 540 to 1000 km. The s600 phase was not analyzed for this station. All records were processed using filters with center frequencies of 0.6, 1.25, and 2.5 Hz. For various reasons, most records could not be processed in the range centered at 5 Hz. The range centered at 0.6 Hz also yielded insufficiently representative data, and their processing results were considered auxiliary.

The discrimination efficiency is characterized in Table 6 and in Fig. 8. Polarization effects are also evident here without the transformation of horizontal components (the azimuths varied from 94° to 102°). The best discrimination quality obtained from the vertical component records was provided by the S_m/P_{n2} parameter in the frequency range centered at 2.5 Hz. The averages of this parameter are –0.398 for explosions and 0.36 for earthquakes, and the respective variances are 0.017 and 0.049. The DQC is 2.14. The best discriminant as constrained by the N–S and E–W components is the Lg/P_{n2} parameter in the ranges centered at 1.25

and 2.5 Hz, respectively. The respective DQCs are 2.5 and 1.89.

RESULTS AND DISCUSSION

A distinctive characteristic of the analysis performed is the selection of seismograms of earthquakes and explosions from a comparatively small area of western China. The main advantage of such an approach is that, in analyzing records of the same station, one can neglect, to a first approximation, the structural differences between various traces in the lithosphere and asthenosphere. On the other hand, only a small amount of records could be selected even over a long period of observation in the area characterized by relatively weak seismicity, and this did not allow us to introduce corrections for the epicentral distances and magnitudes of the events.

The physical interpretation of the UNE discrimination using the amplitude ratios of regional phases lies in the fact that, during nuclear explosions, a smaller amount of energy is radiated in the form of S waves as
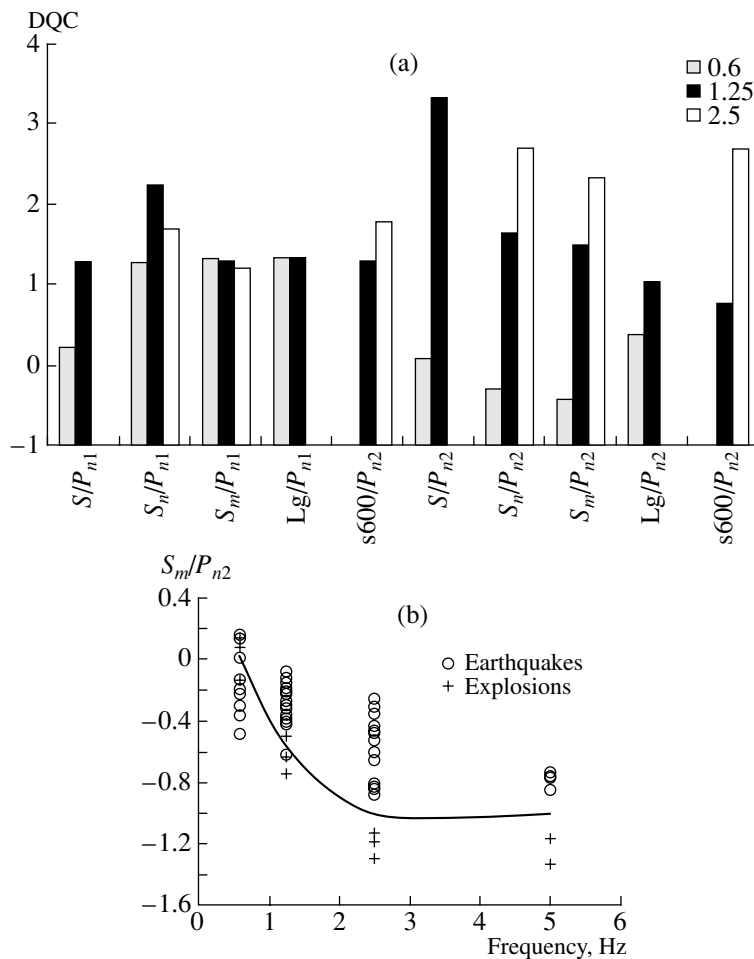
Fig. 7. (a) DQC values for various types of amplitude ratios. (b) Distribution of the S_m/P_{n2} ratio for explosions and earthquakes. ZRN station, Z channel.

compared with earthquakes. In this work, we used a few types of discrimination parameters characterizing S waves, so that their joint analysis reduced the probability of errors.

The small amount of UNE records did not allow us to determine reliably the shape of the distribution curves of the amplitude ratios studied. There is no evidence supporting the assumption that the distribution curves from explosions and earthquakes are similar in shape. For this reason, all statistical calculations were carried out without approximation of the distribution curves. Consequently, it was impossible to determine the probability of discrimination errors from the entire assembly. For most stations considered, sample estimation of the efficiency of the method proposed in this work yielded a nearly 100% reliability of explosion discrimination for all selected events, which should undoubtedly diverge from entire assembly estimates.

We should emphasize that the subdivision of the P_n wave group into two phases plays an essential role in our method. At the first stage, we did not perform this subdivision, and the discrimination between explosions

and earthquakes was appreciably less efficient; moreover, the relevant optimum frequency ranges significantly differed for various stations. Attempts to clear up the reasons of such differences resulted in the subdivision of the P_n group into two components.

The use of the P_{n1} phase generally showed its low efficiency at all stations considered. On the other hand, the parameters of the X/P_{n2} type gave much higher DQC values and a lower number of errors as compared with the parameters of the X/P_n type. Moreover, the diversity of the frequency ranges favorable to the UNE discrimination was significantly reduced for various stations. The S_m/P_{n2} and S_n/P_{n2} parameters were found to be most efficient for the vertical component in the ranges centered at 2.5 and 5 Hz. The amplitude ratios of the Lg code (s300, s450, and s600) to the P_{n2} phase measured in horizontal components were found to be more efficient in the range centered at 1.25 Hz. The Lg/P_{n2} parameter is less stable in this respect and is intermediate in efficiency.
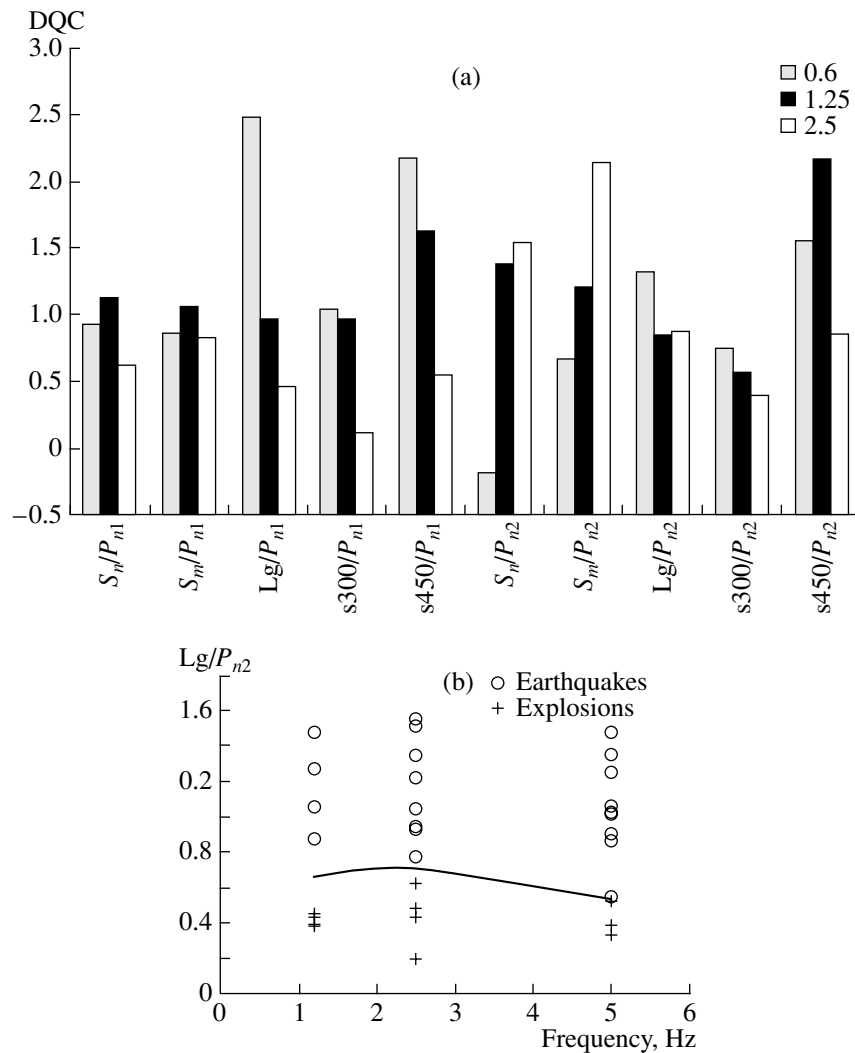
Fig. 8. (a) DQC values for various types of amplitude ratios (Z channel). (b) Distribution of the Lg/P_{n2} ratio for explosions and earthquakes (E–W channel). PDG station.

The differences between the most efficient frequency ranges of various parameters is supposedly related to the following circumstances. Kopnichev [1985] and Kopnichev and Arakelyan [1988] showed that the short-period Lg coda is mainly formed by S waves penetrating into the upper mantle. The paths of the S_m, S_n, and Lg waves in the most absorptive and scattering medium (lithosphere and asthenosphere) are evidently shorter than those of the corresponding phases in the Lg coda (in particular, this is demonstrated by a monotonic increase in the dominating periods with increasing record time). Short-period waves attenuate in the crust and upper mantle considerably stronger than P waves (for this reason, S waves with a frequency of about 1 Hz are absent at teleseismic distances [Kopnichev, 1985]). In this connection, the P wave contribution to the Lg wave and, to a great extent, to its coda increases at relatively high frequencies

(Fig. 5), and this results in a decrease in the discrimination efficiency. On the other hand, S-waves dominate in the S_m and S_n phases at relatively high frequencies (2.5 and 5 Hz), which results in a high quality of discrimination between explosions and earthquakes.

The efficient discrimination between explosions and earthquakes within separate frequency ranges is promising for the application of this method to the development of reliable UNE discriminants in poorly studied areas (Pakistan and India), because the Joint seismological expedition of the Schmidt United Institute of Physics of the Earth, Russian Academy of Sciences possesses a unique archive of records of earthquakes in these regions accumulated over a long time. The problem of discriminating the UNEs detonated at the Indian and Pakistan test sites will be discussed in a special paper.

CONCLUSIONS

(1) The characteristics of short-period wave fields were studied from data on 18 LTS UNEs and 29 earthquakes in western China recorded at four seismic stations at epicentral distances of 540–2300 km between 1969 and 1999.

(2) The amplitude ratios of various regional phases formed by *S* and *P* waves were analyzed in four narrow frequency ranges from an interval of 0.5–6 Hz.

(3) The most efficient parameters and frequency ranges, providing the best discrimination between explosions and earthquakes at various stations, are established.

(4) The discovered effects are interpreted in terms of a concept consistent with the results of observations.

ACKNOWLEDGMENTS

REFERENCES

Antonova, L.V., Aptikaev, F.F., Kurochkina, R.I., *et al.*, *Eksperimental'nye seismicheskie issledovaniya nedr Zemli* (Experimental Seismic Studies of the Earth's Interiors), Moscow: Nauka, 1978.

Aranovich, Z.I., Kirnos, D.P., Tokmakov, V.A., *et al.*, Main Types of Seismometers, in *Apparatura i metodika seismometricheskikh nablyudenii v SSSR* (Instrumentation and Methods of Seismic Observations in the USSR), Moscow: Nauka, 1974, pp. 43–117.

Belyashova, N.N. and Malakhova, M.N., The Seismological Network of the National Nuclear Center, Republic of Kazakhstan, as a Constituent of the International System of the Nuclear Test Monitoring, *Vestnik NYaTs RK Geofizika i problemy nerasprostraneniya* (Bulletin of the National Nuclear Center, Republic of Kazakhstan: Geophysics and Problems of Non-Proliferation), Kurchatov, 2000, pp. 13–16.

Brulev, Yu.V., Krylov, G.G., Nersesov, I.L., *et al.*, Instrumentation of Regional Seismic Studies, in *Instrumental'nye sredstva seismicheskikh nablyudenii. Seismicheskie pribory* (Instrumental Techniques of Seismic Observations. Seismic Instruments), Moscow: Nauka, 1980, issue 13, pp. 138–153.

Fan, G. and Lay, T., Statistical Analysis of Irregular Wave-Guide Influences on Regional Seismic Discriminants in China, *Bull. Seismol. Soc. Am.*, 1998a, vol. 88, no. 1.

Fan, G. and Lay, T., Regionalized Versus Single-Station Wave-Guide Effects on Seismic Discriminants in Western China, *Bull. Seismol. Soc. Am.*, 1998b, vol. 88, no. 5, pp. 1260–1274.

Fan, G. and Lay, T., Statistical Analysis of Irregular Wave-Guide Influences on Regional Seismic Discriminants in China: Additional Results for P_n/S_n, P_n/Lg, and Pg/S_n, *Bull. Seismol. Soc. Am.*, 1998c, vol. 88, no. 6, pp. 1504–1510.

Hartse, H.E., Taylor, S.R., Phillips, W.S., *et al.*, A Preliminary Study of Regional Seismic Discrimination in Central Asia with Emphasis on Western China, *Bull. Seismol. Soc. Am.*, 1997, vol. 87, no. 3.

Kedrov, O.K. and Lyuke, E.I., Discrimination between Nuclear Explosions and Earthquakes in Eurasia from Seismic Data at Regional Distances, *Fiz. Zemli*, 1999, no. 9, pp. 52–75.

Kim, W.Y., Simpson, D.W., and Pichards, P.G., Discrimination of Earthquakes and Explosions in the Eastern United States Using Regional High-Frequency Data, *Geophys. Res. Lett.*, 1993, vol. 20, no. 14, pp. 1507–1510.

Kopnichev, Yu.F., *Korotkoperiodnye seismicheskie volnovye polya* (Short-Period Seismic Wave Fields), Moscow: Nauka, 1985.

Kopnichev, Yu.F. and Arakelyan, A.R., On the Origin of the Short-Period Seismic Fields at Distances of up to 3000 km, *Vulkanol. Seismol.*, 1988, no. 4, pp. 77–92.

Phillips, W.S., Hartse, H.E., Taylor, S.R., *et al.*, Regional Phase Amplitude Tomography for Seismic Verification in China, *21st Seismic Research Symposium*, Las Vegas, 1999, pp. 216–225.

Rogers, A.J., Lay, T., Walter, W.R., and Mayeda, K.M., A Comparison of Regional Phase Amplitude Ratio Measurement Techniques, *Bull. Seismol. Soc. Am.*, 1997, vol. 87, no. 6.

Taylor, S.R., Velasco, A.A., Hartse, H.E., and Phillips, W.S., Amplitude Corrections for Regional Seismic Discriminants, *21st Seismic Research Symposium*, Las Vegas, 1999, pp. 646–655.

Zapol'skii, K.K., Frequency-Selective Seismic Stations, *Eksperimental'naya seismologiya* (Experimental Seismology), Moscow: Nauka, 1971, pp. 20–36.